Available online at www.sciencedirect.com

SciVerse ScienceDirect

journal homepage: www.elsevier.com/locate/jmbbm

Research paper

Effects of hydroxyapatite reinforcement on the architecture and mechanical properties of freeze-dried collagen scaffolds

*Robert J. Kane, Ryan K. Roeder**

Department of Aerospace and Mechanical Engineering, Bioengineering Graduate Program, University of Notre Dame, Notre Dame, IN, 46556, USA

ARTICLE INFO

Article history:
Published online 25 September 2011

Keywords:
Collagen
Composite
Hydroxyapatite
Tissue engineering scaffold
Freeze-dried
Synthetic bone graft substitute

ABSTRACT

Freeze-dried collagen scaffolds reinforced with hydroxyapatite (HA) are of clinical interest for synthetic bone graft substitutes and tissue engineering scaffolds, but a systematic evaluation of the effects of the HA reinforcement weight fraction and morphology on the mechanical properties is lacking. Therefore, freeze-dried collagen scaffolds were reinforced with either HA whiskers or an equiaxed HA powder at 1:1, 1:2, or 1:4 collagen:HA by weight (which corresponded to approximately 28, 44, and 61 vol% HA, respectively) to investigate the effects of the HA reinforcement weight fraction and morphology on the architecture and compressive mechanical properties. All scaffolds exhibited a highly elongated linear pore structure containing 90%–96% porosity, which decreased with increased HA content, and a pore width of ~50 μm. HA reinforcement resulted in up to a ten-fold increase in compressive modulus at high reinforcement levels (~200 kPa at 1:4 collagen:HA by weight) compared to scaffolds with no reinforcement or low reinforcement levels (~20 kPa at 1:1 collagen:HA by weight). This effect could not be explained by the concomitant decrease in the scaffold porosity (from 95% to 90%) with HA reinforcement, which could only account for up to a two-fold increase in compressive modulus. At moderate reinforcement levels (1:2 collagen:HA by weight), HA whisker reinforced scaffolds exhibited a nearly four-fold greater modulus compared to the equiaxed HA powder, while there were no differences with the HA reinforcement morphology at high and low reinforcement levels. Therefore, the elongated morphology of HA whiskers enabled a reinforcing effect at a lower level of reinforcement compared to a conventional, equiaxed HA powder.

1. Introduction

Over 500,000 bone graft procedures are performed each year in the United States making bone the most transplanted tissue. Autografts are the "gold standard", but are limited in size, shape, and availability (Arrington et al., 1996; Greenwald et al., 2001). Moreover, autograft harvesting can result in donor site morbidity, especially as patient age increases (Arrington et al., 1996; Seiler and Johnson, 2000). Allograft tissue alleviates size and shape constraints, but is limited by donor tissue availability and an increased risk of immunogenic response, disease transmission, and infection

* Correspondence to: Department of Aerospace and Mechanical Engineering, Bioengineering Graduate Program, 148 Multidisciplinary Research Building, University of Notre Dame, Notre Dame, IN, 46556, USA. Tel.: +1 574 631 7003; fax: +1 574 631 2144.
E-mail address: rroeder@nd.edu (R.K. Roeder).

1751-6161/$ - see front matter © 2011 Elsevier Ltd. All rights reserved.
doi:10.1016/j.jmbbm.2011.09.010

(Greenwald et al., 2001; Lord et al., 1988). Therefore, the limitations associated with autograft and allograft tissue have motivated extensive research and commercial product development for synthetic bone graft substitutes.

Synthetic bone graft substitutes available for clinical use are under continuous change, but currently include: calcium sulfate (e.g., Osteoset®, Wright Medical), porous hydroxyapatite (Pro-Osteon®, Biomet; FRIOS Algipore®, Dentsply; Bio-Oss®, Osteohealth), porous silicon substituted hydroxyapatite (Actifuse®, Baxter Healthcare), porous beta-tricalcium phosphate (ChronOS, Synthes; Vitoss®, Orthovita), calcium phosphate cements (Norian SRS®, Synthes; BoneSource®, Stryker; α-BSM®, ETEX), collagen sponges loaded with bone morphogenetic protein (InFuse®, Medtronic Somafor Danek; OP-1®, Olympus Biotech), and hydroxyapatite reinforced porous collagen (CopiOs®, Zimmer; Healos®, DePuy), among others (De Long et al., 2007; Friedlaender et al., 2006) and not including demineralized bone matrix. Each graft substitute offers advantageous properties, but also suffers from its own limitations. Calcium phosphates provide bioactivity, but are brittle, particularly in highly porous scaffolds which may also exhibit low strength. Collagen materials alone lack the stiffness and strength required to bear load prior to or during healing. An ideal or widely applicable synthetic bone graft substitute does not yet exist.

A logical approach for the design of a synthetic bone graft substitute is to mimic the structure and composition of natural bone tissue, potentially resulting in properties similar to graft tissue without the associated limitations and risks. The extracellular matrix (ECM) of bone tissue is a composite composed of type I collagen fibers reinforced with calcium-deficient hydroxyapatite (HA) crystals which are elongated and plate-like (Rho et al., 1998). Therefore, dense (Du et al., 2000; Itoh et al., 2002; Kikuchi et al., 2001; TenHuisen et al., 1995) and porous (Al-Munajjed et al., 2009; Gelinsky et al., 2008; Liu et al., 2003; Tampieri et al., 2003; Wahl et al., 2007; Wang et al., 1995; Yunoki et al., 2007) collagen–HA composites have been investigated for synthetic bone graft substitutes and bone tissue engineering scaffolds. Collagen-HA scaffolds are typically prepared by freeze drying to achieve high levels of interconnected porosity (~80%–99%) required for cell infiltration, nutrient transport, vascularization, and tissue regeneration (Al-Munajjed et al., 2009; Cunniffe et al., 2010; Harley et al., 2010; Jones et al., 2010; Lyons et al., 2010; Wahl et al., 2007; Yunoki et al., 2007). Moreover, the porosity, pore size, and pore morphology of freeze-dried collagen scaffolds can be tailored by controlling the freezing rate, freezing temperature, and collagen concentration (Harley et al., 2007, 2010; O'Brien et al., 2004, 2005; Schoof et al., 2001; Tierney et al., 2009; Wahl et al., 2007; Yunoki et al., 2010).

The mechanical properties of freeze-dried collagen–HA scaffolds are typically investigated in unconfined uniaxial compression but comparisons between studies are complicated by differences in the HA content, HA morphology, porosity, pore architecture, and fabrication methods (Al-Munajjed and O'Brien, 2009; Cunniffe et al., 2010; Gelinsky et al., 2008; Gleeson et al., 2010; Harley et al., 2010; Yunoki et al., 2007). The inherently thin struts within a freeze-dried collagen scaffold result in a low apparent compressive modulus typically reported within the range of 1–150 kPa. The maximum reported compressive modulus for a freeze-dried collagen–HA scaffold was ~280 kPa in an anisotropic scaffold containing highly aligned struts (Yunoki et al., 2007). A systematic evaluation of the effects of the HA reinforcement weight fraction and morphology on the mechanical properties of freeze-dried collagen scaffolds is lacking.

Therefore, the objective of this study was to investigate the effects of the HA reinforcement weight fraction and morphology on the architecture and compressive mechanical properties of freeze-dried collagen scaffolds. Scaffolds were reinforced with either HA whiskers or an equiaxed HA powder at 1:1, 1:2 and 1:4 collagen:HA by weight. The scaffold porosity and pore size were also measured to account for possible concomitant effects on the mechanical properties.

2. Materials and methods

2.1. *Collagen purification*

Soluble type I collagen was extracted from bovine dermis using acid extraction and salt fractionation (Trelstad, 1982; Huang-Lee and Nimni, 1993). Bovine dermal tissue was trimmed of hair and excess fat. Strips of tissue, weighing 500 g and measuring ~10 × 50 mm, were defatted in 1 L of 50/50 chloroform/methanol by volume for 8 h and washed for 2 h each in 100% methanol, 50% methanol in water by volume, and finally physiological phosphate buffered saline (PBS). Defatted dermal tissue strips were then placed in 1.5 L of 0.5 M acetic acid and blended for 5 min in a commercial blender (Model 909, Hamilton Beach/Procter-Silex, Inc., Washington, NC). Porcine pepsin (P7000, Sigma-Aldrich, Milwaukee, WI) was added at a concentration of 2 mg/mL to increase the fraction of extractable soluble collagen. Pepsin preferentially attacks the globular ends of the collagen proteins, breaking crosslinks that bind collagen molecules to each other. Pepsin can increase the extractable yield by 400% and the resulting collagen displays lower immunogenicity compared to collagen not treated with pepsin (Trelstad, 1982). The acid solution was adjusted to a pH of 2.5 with HCl for optimum pepsin activity and incubated at 4 °C for 24 h.

After acid extraction, the solution was centrifuged at 5000 g for 1 h to remove all non-soluble collagen fragments. The supernatant contained 5–10 mg/mL of soluble type I collagen. Other minor contaminants likely included residual elastin, type III collagen, and keratin. Type I collagen was separated by adding NaCl to a concentration of 2.5 M to induce precipitation. The precipitated collagen was collected by centrifugation at 7500 g for 1 h, re-dissolved in 0.1 M acetic acid, centrifuged again at 7500 g for 1 h, and the remaining precipitate was discarded. The resulting supernatant was nearly pure type I collagen as demonstrated by sodium dodecyl sulfate polyacrylamide gel electrophoresis (SDS-PAGE) using a 10% acrylimide gel and comparing the sample profile to a commercial protein standard (Fig. 1). The final collagen solution was freeze-dried and stored at −20 °C until further use.

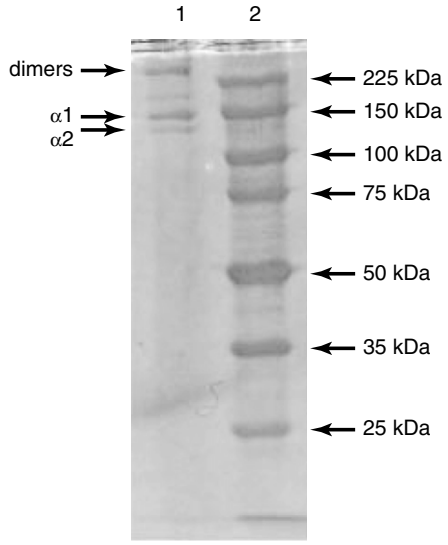

Fig. 1 – SDS-PAGE gels for (lane 1) collagen purified from bovine dermis and (lane 2) protein standards. Note that the faint line at ~30 kDa in lane 1 is equal to the cutoff limit of the dialysis tubing used during purification.

2.2. *Hydroxyapatite reinforcements*

Single crystal HA whiskers were precipitated by a hydrothermal reaction using the chelate decomposition method, allowing the morphology to be controlled by adjusting the heating rate, stirring rate, and chelating acid, among other variables (Roeder et al., 2006). The synthesis conditions for the whiskers used in this study resulted in a mean (±standard deviation) length and aspect ratio of 18 (8.9) μm and 7.9 (3.4), respectively, as described in detail elsewhere (Roeder et al., 2003).

An equiaxed HA powder was obtained commercially (Product #21221, Fluka Chemical Co., Buchs, Switzerland). The as-received powder was ground using a mortar and pestle to minimize agglomerates, and stored at 90 °C to remove residual moisture. The mean (±standard deviation) particle diameter of this powder was previously reported as 1.3 (0.4) μm (Roeder et al., 2003), which was comparable to the width of the whiskers.

2.3. *Scaffold preparation*

Scaffolds were prepared by dispersing previously freeze-dried collagen at a concentration of 50 mg/mL in 30 mL of 0.1 M acetic acid in de-ionized water. This collagen concentration was the maximum attainable while still maintaining an even dispersion. Mixing was performed using a commercial blender with a shear mixer attachment for 2 min, followed by a 10 min rest, and another 2 min of mixing. HA reinforcements were then added at 1:1, 1:2, or 1:4 collagen:HA by weight, and the solution was mixed for another 2 min. The final collagen–HA solution was degassed in a vacuum desiccator for 30 min. Note that the collagen solution was maintained at ~4 °C during all preparation procedures.

The collagen–HA solution was poured into individual cylindrical silicone molds, 10 mm in diameter and 7.5 mm in height, that were placed onto a stainless steel pan for freeze-drying. The pan and molds were placed into a freeze-drier (FreeZone Triad, Labconco Inc., Kansas City, MO) on a specimen platen cooled to −80 °C, which generated a high temperature gradient and ice crystals perpendicular to the bottom surface of the mold. Scaffolds were lyophilized at 1 kPa and −30 °C for 24 h, and stored at 0 °C until further use.

All scaffolds in this study were crosslinked using a dehydrothermal treatment (DHT), gradually heating to 105 °C at 1 kPa over 6 h, and holding at 105 °C for 24 h. DHT has been extensively characterized in collagen and collagen–HA scaffolds (Haugh et al., 2009; Ma et al., 2003; Pieper et al., 1999; Tierney et al., 2009). Crosslinking by DHT results in an increased elastic modulus similar to that produced by chemical crosslinking agents such as gluteraldehyde (GTA) but without toxicity and immunogenic concerns (Tierney et al., 2009).

Pure collagen scaffolds were prepared as a control, and six groups were reinforced with either HA whiskers or powder at 1:1, 1:2, and 1:4 collagen:HA by weight, which corresponded to approximately 28, 44, and 61 vol% HA, respectively. Therefore, scaffolds at 1:2 and 1:4 collagen:HA by weight approximated lower and upper bounds for the mineral content present in the ECM of bone (Hernandez et al., 2001; Zioupos et al., 2008). Nine scaffolds were prepared for each of the seven experimental groups ($n = 9$). Seven scaffolds from each group were used for measuring mechanical properties and porosity. Two scaffolds from each group were used for histology and scanning electron microscopy, respectively, as described below.

2.4. *Microstructural characterization*

The scaffold porosity and pore width were measured in order to determine whether differences in mechanical properties were due to changes in the scaffold material properties or the scaffold architecture. The porosity of scaffolds from each experimental group (n = 3–5 per group) was determined from the ratio of the measured apparent scaffold density and calculated theoretical scaffold density. The apparent scaffold density was calculated from the ratio of the dry scaffold weight, measured using a mass balance (±0.001 g), and the hydrated scaffold volume, measured using digital calipers (±0.01 mm). After mechanical testing, scaffolds were ashed at 800 °C for 24 h to pyrolize the collagen. The mass of HA was measured as the ash weight and the mass of collagen was calculated as the difference in the dry scaffold weight and ash weight. The theoretical scaffold density was calculated from the mass of collagen and HA in each scaffold, assuming a density of 1.23 g/cm^3 for collagen (Black and Mattson, 1982) and 3.156 g/cm^3 for HA (Hing et al., 1999).

The mean pore width of one scaffold from each experimental group was measured by histology. As-prepared collagen–HA scaffolds were embedded in paraffin and sectioned using a sledge microtome (SM2010, Leica GmbH, Wetzlar, Germany) normal to the direction of ice crystal formation during freeze drying. Twenty serial sections, 30–60 μm in thickness and spaced ~200 μm apart, were prepared for each scaffold. Each section was transferred to a silanized glass slide, deparaffinized, and stained with aniline blue to

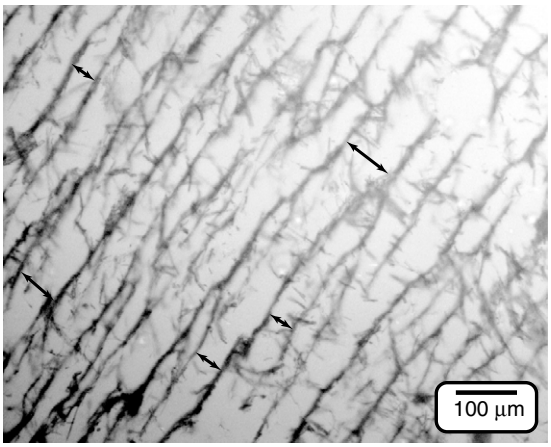

Fig. 2 – Transmitted light micrograph showing a transverse section of a freeze-dried collagen scaffold reinforced with HA whiskers at 1:2 collagen:HA by weight. Arrows show measurements of the strut spacing, or pore width, at five random locations in the section.

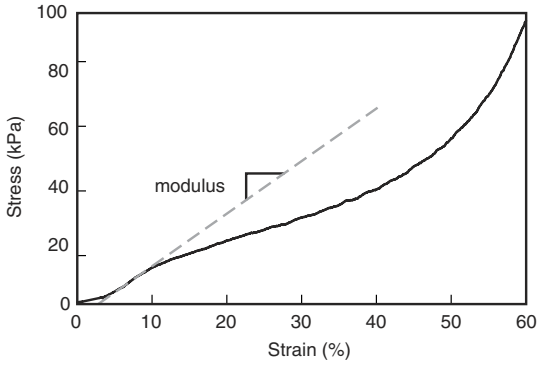

Fig. 3 – Representative stress–strain curve for unconfined uniaxial compression of a freeze-dried collagen scaffold reinforced with HA whiskers at 1:4 collagen:HA by weight. The compressive modulus was calculated by linear least squares regression using the segment of the apparent stress–strain curve exhibiting the greatest slope over a 3% strain range within all data between zero and 20% strain.

label collagen. Scaffold sections were imaged at 50× magnification using transmitted light microscopy (Eclipse ME600, Nikon Instruments Inc., Melville, NY). The mean pore width for each scaffold section was determined using a MATLAB (MathWorks, Inc., Natick, MA) script to generate five random points in the image. The strut spacing at each point was then measured using and a mean strut spacing was calculated for each section (Fig. 2). Therefore, the mean pore width for each scaffold represented a total of 100 measurements distributed evenly throughout the scaffold volume.

One specimen from each experimental group was freeze-fractured and imaged using scanning electron microscopy (Evo 50, LEO Microscopy Ltd, Cambridge, UK) with an accelerating voltage of 10–15 kV and a working distance of 7–10 mm. Scaffolds were coated with 10 nm iridium by sputter deposition prior to imaging (208HR, Cressington Scientific Instruments Ltd., Watford, UK).

2.5. *Mechanical characterization*

Scaffolds were loaded in unconfined uniaxial compression at a rate of 0.01 mm/s to ~75% strain using an electromagnetic test instrument (ElectroForce 3300, Bose Corp., Eden Prairie, MN). All scaffolds were rehydrated for 1 h in PBS prior to loading and were maintained at ambient temperature in PBS during loading. Load and displacement data were collected at a rate of 10 Hz using a 25 lb load cell and linear variable displacement transducer, respectively. Apparent stress and strain were calculated based upon the dimensions of the rehydrated scaffold prior to loading using digital calipers (±0.01 mm). The compressive modulus was calculated by linear least squares regression using the segment of the apparent stress–strain curve exhibiting the greatest slope over a 3% strain range within all data between zero and 20% strain (Fig. 3). This approach was used instead of a fixed strain range because the elastic collapse stress and strain increased with increasing HA reinforcement.

2.6. *Statistical methods*

One-way and two-way analysis of variance (ANOVA) (JMP 8.1, SAS Inc, Cary, NC) were used to investigate the effects of the HA reinforcement weight fraction and morphology on the porosity, pore width, and compressive modulus of scaffolds. *Post-hoc* comparisons were performed using Tukey's HSD test. The ash weight fraction of HA reinforcements was compared to the designed weight fraction using a paired *t*-test. The level of significance for all tests was set at $p < 0.05$.

3. Results

The designed HA weight fraction was not statistically different from the HA weight fraction measured from ashed scaffolds ($p = 0.93$, paired *t*-test), confirming the preparation methods. The visual appearance of all as-prepared scaffolds was similar regardless of the HA reinforcement level. Histological sections (Fig. 2) and SEM micrographs of freeze-fractured scaffolds (Fig. 4(a)) showed a highly elongated linear pore structure. HA particles or whiskers were observed on scaffold strut surfaces at higher magnification (Fig. 4(b) and (c)). In the case of HA whisker reinforced scaffolds, the freezing process appeared to preferentially align whiskers in the direction of ice crystal propagation along the mechanical loading axis (Fig. 4(c)). All scaffolds contained numerous transverse cross-struts bridging the elongated pores, but their morphology varied depending upon the HA reinforcement weight fraction and morphology. Cross-struts in unreinforced scaffolds appeared thin and ropelike (Fig. 5(a)). Scaffolds reinforced with HA powder contained small HA particles incorporated into the cross-struts, which otherwise appeared similar to the cross-struts in unreinforced scaffolds (Fig. 5(b)). However, cross-struts in HA whisker reinforced scaffolds were thicker and the pore space was often bridged by HA whiskers (Figs. 4(b) and 5(c)).

All scaffolds contained 90%–96% porosity and a pore width of ~50 μm (Fig. 6). The mean (±standard deviation) porosity

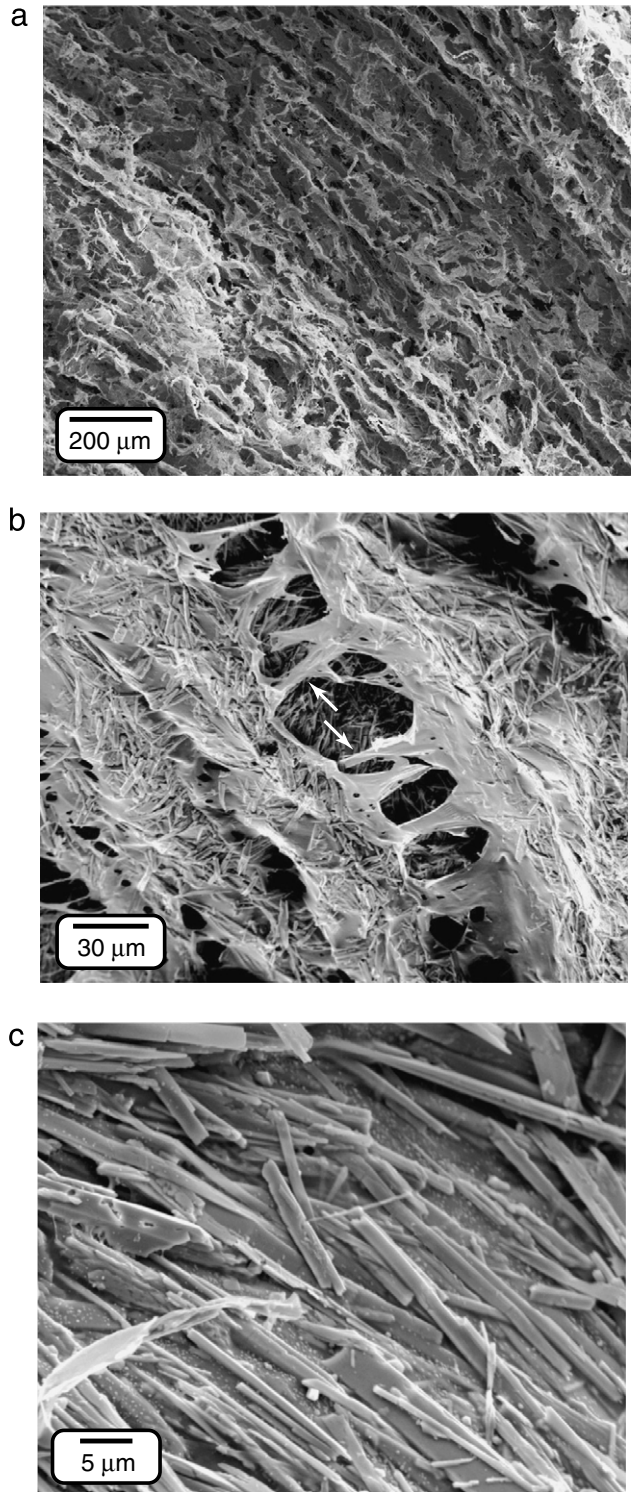

Fig. 4 – SEM micrographs of freeze-fractured transverse cross-sections from representative freeze-dried collagen scaffolds reinforced with HA whiskers at 1:2 collagen:HA by weight, showing the hierarchical structure: (a) elongated and aligned pores separated by thin struts, (b) transverse cross-struts between axial struts, and (c) HA whiskers exposed and aligned on strut surfaces. Arrows in (b) highlight individual HA whiskers which bridge the pore space.

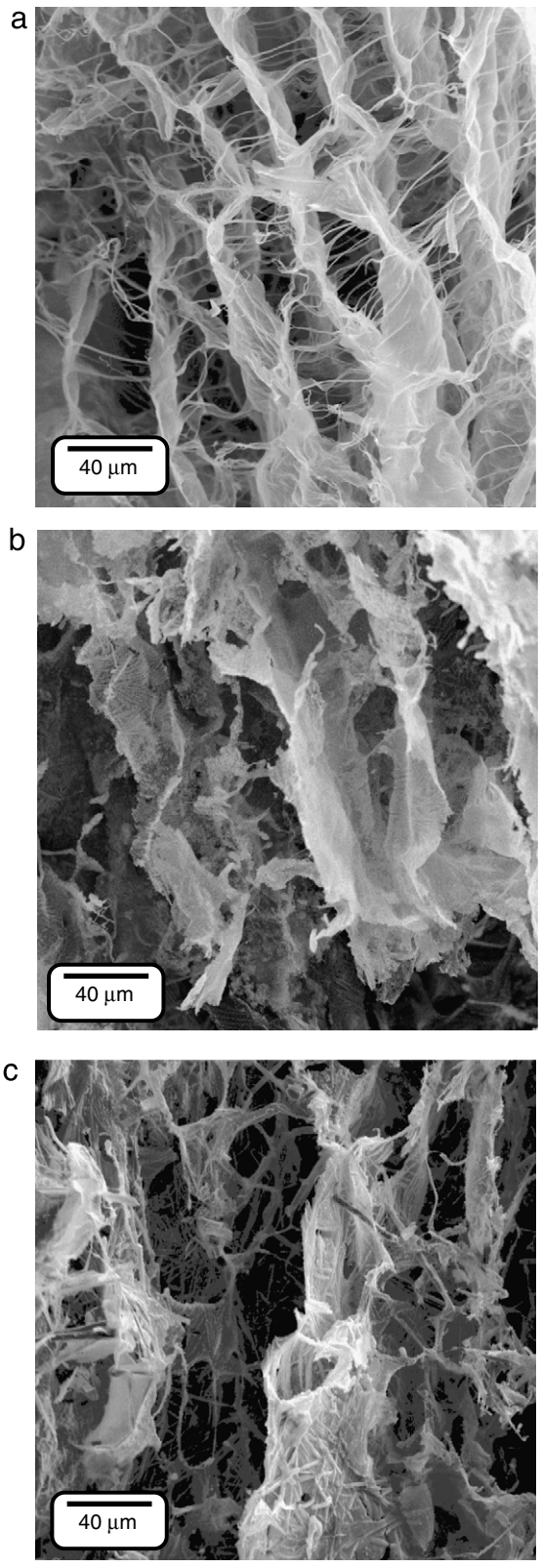

Fig. 5 – Representative SEM micrographs of freeze-fractured transverse cross-sections showing the effects of HA reinforcement on the transverse cross-struts bridging pores for freeze-dried collagen scaffolds with (a) no HA reinforcement, (b) HA powder at 1:4 collagen:HA by weight, and (c) HA whiskers at 1:4 collagen:HA by weight.

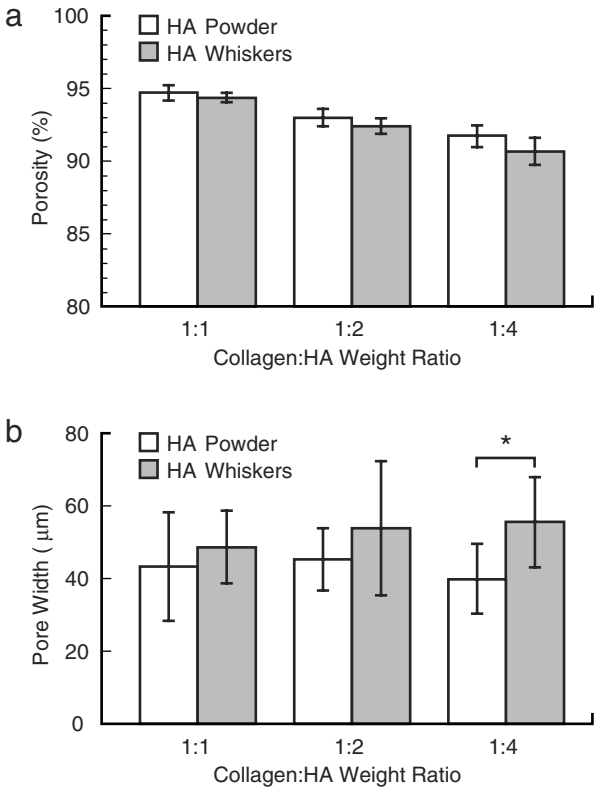

Fig. 6 – The mean (a) porosity and (b) pore width of freeze-dried collagen scaffolds reinforced with HA whiskers or powder at 1:1, 1:2 and 1:4 collagen:HA by weight. Error bars show one standard deviation. Porosity decreased with an increased HA reinforcement weight fraction ($p < 0.0001$, ANOVA) and for HA whiskers compared to HA powder ($p < 0.05$, ANOVA), but differences between the HA morphology as a given collagen:HA weight ratio were not statistically significant. The pore width was not affected by the HA reinforcement weight fraction ($p = 0.38$, ANOVA), but increased for HA whiskers compared to HA powder ($p < 0.0001$, ANOVA). The mean pore width of HA whisker reinforced scaffolds was significantly greater than HA powder scaffolds at 1:4 collagen:HA by weight ($p < 0.005$, Tukey's HSD), but all other differences were not statistically significant. $^{*}p < 0.005$ (Tukey's HSD), HA whiskers vs. powder.

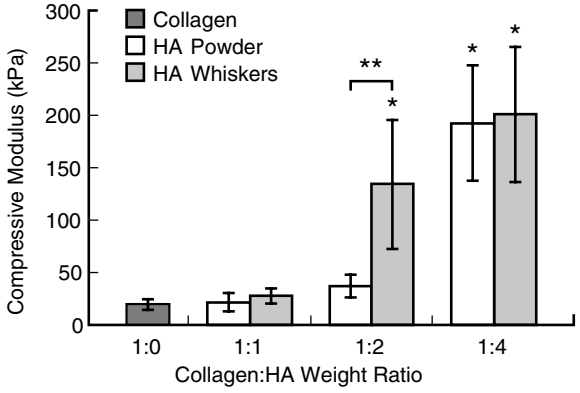

Fig. 7 – The apparent mean compressive modulus of freeze-dried collagen scaffolds reinforced with HA whiskers or powder at 1:0, 1:1, 1:2, and 1:4 collagen:HA by weight ($n = 7$/group). Error bars show one standard deviation. The modulus increased with increased HA reinforcement weight fraction ($p < 0.0001$, ANOVA). Scaffolds reinforced with HA whiskers at 1:2 collagen:HA by weight, and either HA whiskers or powder at 1:4 collagen:HA by weight, exhibited an increased compressive modulus compared to the collagen control ($p < 0.0001$, Tukey's HSD). The compressive modulus was increased for HA whisker compared to HA powder reinforcement overall ($p < 0.01$, ANOVA), but the difference at a given weight fraction was only statistically significant at 1:2 collagen:HA by weight ($p < 0.001$, Tukey's HSD). $^{*}p < 0.0001$ (Tukey's HSD) vs. collagen control. $^{**}p < 0.001$ (Tukey's HSD), HA whiskers vs. powder.

of collagen scaffolds was 96.2 (0.5)%. The mean scaffold porosity decreased with increased HA reinforcement weight fraction ($p < 0.0001$, ANOVA), but the magnitude of the effect was relatively small (Fig. 6(a)). The mean scaffold porosity was also decreased for HA whisker compared to HA powder reinforcements overall ($p < 0.05$, ANOVA), but differences at a given HA weight fraction were not statistically significant. The mean pore width was not affected by the HA reinforcement weight fraction ($p = 0.38$, ANOVA) (Fig. 6(b)). The mean pore width was increased for HA whisker compared to HA powder reinforcements overall ($p < 0.0001$, ANOVA), and at 1:4 collagen:HA by weight ($p < 0.005$, Tukey's HSD), but these differences were relatively small in magnitude. All group means were within 17% of the overall mean (±standard deviation) pore width, which was 47.9 (12.6) μm.

Scaffolds exhibited stress–strain curves with characteristics indicative of elastomeric cellular solids, including a linear elastic region, elastic collapse stress, elastic buckling region, and finally densification (Fig. 3). The compressive modulus increased with increased HA reinforcement weight fraction ($p < 0.0001$, ANOVA) (Fig. 7). Scaffolds reinforced with HA whiskers at 1:2 collagen:HA by weight, and either HA whiskers or powder at 1:4 collagen:HA by weight, exhibited an increased compressive modulus compared to the collagen control ($p < 0.0001$, Tukey's HSD). The compressive modulus was increased for HA whisker compared to HA powder reinforcement overall ($p < 0.01$, ANOVA). However, the difference at a given weight fraction was only statistically significant at 1:2 collagen:HA by weight ($p < 0.001$, Tukey's HSD).

4. Discussion

The objective of this study was to investigate the effects of the HA reinforcement weight fraction and morphology on the architecture and compressive mechanical properties of freeze-dried collagen scaffolds. Freeze-dried collagen scaffolds were reinforced with up to 80 wt% (~61 vol%) HA, which was similar to the maximum HA reinforcement content reported for other collagen–HA scaffolds (Cunniffe et al., 2010; Harley et al., 2010; Yunoki et al., 2007), as well

as the ECM of bone tissue (Hernandez et al., 2001; Zioupos et al., 2008). HA reinforcement of collagen scaffolds resulted in up to a ten-fold increase in compressive modulus at high reinforcement levels (1:4 collagen:HA by weight, or ~61 vol% HA), but little or no increase at lower reinforcement levels (1:1 collagen:HA by weight, or ~28 vol% HA) (Fig. 7). At 1:2 collagen:HA by weight, HA whisker reinforcement resulted in more than a six-fold increase in compressive modulus, while HA powder reinforcement did not significantly increase the compressive modulus. Therefore, the results of this study suggest that the minimum level of HA reinforcement required to significantly increase the compressive modulus of freeze-dried collagen scaffolds is 1:4 collagen:HA by weight (~61 vol% HA) for HA powder, but only 1:2 collagen:HA by weight (~44 vol% HA) for HA whiskers.

Differences in the compressive modulus of scaffolds in this study were mostly, if not solely, due to the HA reinforcement weight fraction and morphology. Changes in the HA weight fraction and morphology resulted in few apparent architectural differences between scaffolds (Figs. 4 and 5), and only non-significant or relatively minor differences in the measured porosity and pore width (Fig. 6). The modulus of highly porous, freeze-dried collagen scaffolds was not dependent on the pore size or width, as expected for an open cell foam, and increased nearly linearly with decreased porosity (Harley et al., 2007). Therefore, using the empirical relative modulus versus density relationship determined by Harley et al. (2007) for isotropic freeze-dried collagen scaffolds, the decrease in porosity from 95% to 90% for scaffolds reinforced with 1:1 and 1:4 collagen:HA by weight would be expected to result in, at most (considering the effects of anisotropy), a two-fold increase in compressive modulus, rather than the ten-fold increase measured in this study (Fig. 7). Furthermore, the effect of the reinforcement morphology and the nonlinear effect of the HA weight fraction on the compressive modulus cannot be explained by a linear relationship between the modulus and scaffold porosity. However, the reinforcement morphology may have influenced the cross-struts.

The increased modulus of scaffolds reinforced with HA whiskers compared to HA powder was expected due to improved load transfer from the matrix to an elongated reinforcement. However, this effect was only statistically significant in scaffolds reinforced with 1:2 collagen:HA by weight (Fig. 7), which was somewhat surprising. A possible explanation was identified in the reinforcement of cross-struts interconnecting the primary plate-like scaffold struts oriented in the direction of loading (Figs. 4 and 5). The primary scaffold struts acted as thin columns (<10 μm thick) susceptible to buckling under load (Harley et al., 2007). Resistance to buckling is readily envisioned to be increased by the presence of cross-struts interconnecting the primary load-bearing struts (Fig. 5). Cross-struts in collagen scaffolds were thin, rope-like collagen strands unable to support a compressive load (Fig. 5(a)). At moderate levels of HA, HA whiskers were able to strengthen the cross-struts and long whiskers were able to bridge pores (Fig. 4(b), arrows). At high levels of HA, HA whisker or powder reinforcements significantly increased the rigidity of all scaffold struts (Fig. 5(b) and (c)).

The maximum compressive modulus obtained in this study was ~200 kPa for collagen scaffolds reinforced with either HA whiskers or powder at 1:4 collagen:HA by weight (Fig. 7). A previous study for collagen scaffolds prepared using similar methods, and reinforced with a nanoscale HA powder at 1:1 and 1:5 collagen:HA by weight, reported a maximum compressive modulus of ~6 kPa (Cunniffe et al., 2010). However, a direct comparison between these studies is difficult since scaffolds prepared by Cunniffe et al. (2010) exhibited a greater porosity (>98%), used a lower collagen concentration (5 mg/mL), and used different HA reinforcements than this study. Another previous study for collagen scaffolds prepared using similar methods, and reinforced with HA powder at 1:4 collagen:HA by weight, reported a maximum compressive modulus of ~140 kPa for isotropic scaffolds and ~280 kPa in the direction of primary struts in anisotropic scaffolds (Yunoki et al., 2007). Again, differences could have been due to any number of factors, including a greater scaffold anisotropy, strut thickness, collagen concentration, DHT temperature, and loading rate in Yunoki et al. (2007) compared to this study. The precise effects of these confounding factors were beyond the scope of the present study, where the objective was to systemically investigate the effects of the HA reinforcement weight fraction and morphology on the compressive mechanical properties, independent of other effects.

The use of HA reinforcements to improve the compressive modulus of freeze-dried collagen scaffolds is important for clinically useful scaffolds that retain their shape during implantation and, ideally, bear mechanical loads after implantation. HA reinforcements were observed to be well-incorporated into the collagen matrix, even at the highest reinforcement level (Fig. 5). However, HA reinforcements were also observed to be exposed on the strut surfaces (Figs. 4 and 5), providing for possible biological activity. Exposed HA reinforcements, and particularly HA whiskers, increased the surface roughness of the scaffold struts, especially compared to the pure collagen control (Fig. 5). Therefore, the enhanced bioactivity and surface roughness provided by HA reinforcements may provide sites for protein adhesion and cell attachment. HA-collagen scaffolds were recently shown to enhance mineralization and bone ingrowth relative to collagen scaffolds (Gleeson et al., 2010; Lyons et al., 2010).

The mean pore width of freeze-dried collagen scaffolds was not affected by the HA reinforcement weight fraction (Fig. 6(b)). Previous work demonstrated that the pore size was controlled primarily by the freezing rate (O'Brien et al., 2004), but there had been no prior investigation for the effects of the HA reinforcement on the scaffold pore size. All scaffolds in this study were frozen at the same temperature and in the same molds. An increased number of HA crystals might be expected to increase the number of ice crystal nucleation sites, resulting in a decreased scaffold pore size with increased HA weight fraction, but no such trend was observed. The observed lack of variation in strut spacing can be partially explained by the use of rapid unidirectional freezing where initial ice crystals are nucleated at the bottom of the slurry, likely at imperfections on the bottom surface of the mold. The ice crystals then

proceeded to rapidly grow upward forming elongated blade-like pores. Therefore, nucleation sites that were present in the collagen–HA solution exhibited little or no influence on ice crystal nucleation. However, if the collagen–HA solution were uniformly cooled to produce an equiaxed pore structure, an increased HA content could increase the number of nucleation sites and reduce the mean pore size.

This study was not without several limitations. A limitation of the pore size measurements was the use of one representative scaffold per experimental group. However, the scaffolds in this study were prepared in individual molds rather than sheets. Therefore, each scaffold was highly reproducible, as supported by the porosity measured for multiple scaffolds (Fig. 6(a)). Moreover, intra-specimen variation in the pore size exhibited no trend relative to histological sections taken across the entire scaffold height ($p > 0.96$, ANOVA). The pore size of unreinforced collagen scaffolds was not measured due to damage during sectioning that was attributed to the lower strength of unreinforced scaffolds and the use of paraffin embedding. However, HA reinforced scaffolds were not affected.

Scaffolds in this study exhibited pore widths ranging from 20 to 90 μm, while pore sizes greater than 100 μm are typically thought to be required for cell infiltration, vascularization, and bone ingrowth (Karageorgiou and Kaplan, 2005). However, HA reinforced freeze-dried collagen scaffolds exhibiting a similar pore architecture to the scaffolds in this study have been reported to support cell infiltration, vascularization, and bone ingrowth (Cunniffe et al., 2010; Gleeson et al., 2010; Jones et al., 2010; Lyons et al., 2010; Pek et al., 2008; Yunoki et al., 2007). Moreover, it is important to recognize that the pore widths reported in this study represent a lower bound of the actual pore size since pore dimensions orthogonal to the measured pore width were substantially greater due to the sheet-like pore structure.

Further work is needed to investigate the effects of the HA reinforcement content and morphology on the response of cells *in vitro*. A recent study reported that the HA content in freeze-dried collagen scaffolds had little influence on the attachment, proliferation, and differentiation of primary human osteoblasts (Jones et al., 2010), but other studies have reported differences with increased HA content (Gleeson et al., 2010). The effects of the reinforcement morphology are unknown and will be the focus of future investigation.

5. Conclusions

Freeze-dried collagen scaffolds were reinforced with either HA whiskers or an equiaxed HA powder at 1:1, 1:2, or 1:4 collagen:HA by weight to investigate the effects of the HA reinforcement weight fraction and morphology on the architecture and compressive mechanical properties. The major conclusions of the study were the following:

(1) HA reinforcement of freeze-dried collagen scaffolds resulted in up to a ten-fold increase in compressive modulus at high reinforcement levels (~200 kPa at 1:4 collagen:HA by weight or ~61 vol% HA) compared to scaffolds with no reinforcement or low reinforcement levels (~20 kPa at 1:1 collagen:HA by weight or ~28 vol% HA).
(2) The scaffold architecture was controlled and shown not to significantly influence the results. HA reinforcement resulted in only non-significant or relatively minor differences in the mean scaffold porosity and pore width.
(3) The elongated morphology of HA whiskers enabled a reinforcing effect at a lower level of reinforcement compared to a conventional, equiaxed HA powder.

Acknowledgments

This research was supported by the US Army Medical Research and Materiel Command (W81XWH-07-1-0662 and W81XWH-09-1-0741).

REFERENCES

Al-Munajjed, A.A., O'Brien, F.J., 2009. Influence of a novel calcium-phosphate coating on the mechanical properties of highly porous collagen scaffolds for bone repair. J. Mech. Behav. Biomed. Mater. 2, 138–146.

Al-Munajjed, A.A., Plunkett, N.A., Gleeson, J.P., Weber, T., Jungreuthmayer, C., Levingstone, T., Hammer, J., O'Brien, F.J., 2009. Development of a biomimetic collagen–hydroxyapatite scaffold for bone tissue engineering using a SBF immersion technique. J. Biomed. Mater. Res. 90B, 584–591.

Arrington, E.D., Smith, W.J., Chambers, H.G., Bucknell, A.L., Davino, N.A., 1996. Complications of iliac crest bone graft harvesting. Clin. Orthop. Relat. Res. 329, 300–309.

Black, J., Mattson, R.U., 1982. Relationship between porosity and mineralization in the Haversian osteon. Calcif. Tissue Int. 34, 332–336.

Cunniffe, G.M., Dickson, G.R., Partap, S., Stanton, K.T., O'Brien, F.J., 2010. Development and characterisation of a collagen nano-hydroxyapatite composite scaffold for bone tissue engineering. J. Mater. Sci. Mater. Med. 21, 2293–2298.

De Long Jr., W.G., Einhorn, T.A., Koval, K., McKee, M., Smith, W., Sanders, R., Watson, T., 2007. Bone grafts and bone graft substitutes in orthopaedic trauma surgery. J. Bone Joint Surg. 89A, 649–658.

Du, C., Cui, F.Z., Zhang, W., Feng, Q.L., Zhu, X.D., de Groot, K., 2000. Formation of calcium phosphate/collagen composites through mineralization of collagen matrix. J. Biomed. Mater. Res. 50A, 518–527.

Friedlaender, G.E., Mankin, H.J., Goldberg, V.M., 2006. Bone grafts and bone graft substitutes. American Academy of Orthopedic Surgeons, Rosemont, IL.

Gelinsky, M., Welzel, P.B., Simon, P., Bernhardt, A., König, U., 2008. Porous three-dimensional scaffolds made of mineralised collagen: preparation and properties of a biomimetic nanocomposite material for tissue engineering of bone. Chem. Eng. J. 137, 84–96.

Gleeson, J.P., Plunkett, N.A., O'Brien, F.J., 2010. Addition of hydroxyapatite improves stiffness, interconnectivity and osteogenic potential of a highly porous collagen-based scaffold for bone tissue regeneration. Eur. Cells Mater. 20, 218–230.

Greenwald, A.S., Boden, S.D., Goldberg, V.M., Khan, Y., Laurencin, C.T., Rosier, R.N., 2001. Bone-graft substitutes: facts, fictions and applications. J. Bone Joint Surg. Am. 83 (Suppl. 2), 98–103.

Harley, B.A., Leung, J.H., Silva, E.C.C.M., Gibson, L.J., 2007. Mechanical characterization of collagen–glycosaminoglycan scaffolds. Acta Biomater. 3, 463–474.

Harley, B.A., Lynn, A.K., Wissner-Gross, Z., Bonfield, W., Yannas, I.V., Gibson, L.J., 2010. Design of a multiphase osteochondral scaffold. II. Fabrication of a mineralized collagen-glycosaminoglycan scaffold. J. Biomed. Mater. Res. 92A, 1066–1077.

Haugh, M.G., Jaasma, M.J., O'Brien, F.J., 2009. The effect of dehydrothermal treatment on the mechanical and structural properties of collagen-GAG scaffolds. J. Biomed. Mater. Res. 89A, 363–369.

Hernandez, C.J., Beaupré, G.S., Keller, T.S., Carter, D.R., 2001. The influence of bone volume fraction and ash fraction on bone strength and modulus. Bone 29, 74–78.

Hing, K.A., Best, S.M., Bonfield, W., 1999. Characterization of porous hydroxyapatite. J. Mater. Sci. Mater. Med. 10, 135–145.

Huang-Lee, L.L.H., Nimni, M.E., 1993. Preparation of type I fibrillar matrices and the effects of collagen concentration on fibroblast contraction. Biomed. Eng. Appl. Basis Comm. 5, 664–675.

Itoh, S., Kikuchi, M., Takakuda, K., Nagaoka, K., Koyama, Y., Tanaka, J., Shinomiya, K., 2002. Implantation study of a novel hydroxyapatite/collagen (HAp/Col) composite into weight bearing sites of dogs. J. Biomed. Mater. Res. 63B, 507–515.

Jones, G.L., Walton, R., Czernuszka, J., Griffiths, S.L., Haj, A.J.E., Cartmell, S.H., 2010. Primary human osteoblast culture on 3D porous collagen–hydroxyapatite scaffolds. J. Biomed. Mater. Res. 94A, 1244–1250.

Karageorgiou, V., Kaplan, D., 2005. Porosity of 3D biomaterial scaffolds and osteogenesis. Biomaterials 26, 5474–5491.

Kikuchi, M., Itoh, S., Ichinose, S., Shinomiya, K., Tanaka, J., 2001. Self-organization mechanism in a bone-like hydroxyapatite/collagen nanocomposite synthesized in vitro and its biological reaction in vivo. Biomaterials 22, 1705–1711.

Liu, L., Zhang, L., Ren, B., Wang, F., Zhang, Q., 2003. Preparation and characterization of collagen–hydroxyapatite composite used for bone tissue engineering scaffold. Artif. Cells Blood Substit. Biotechnol. 31, 435–448.

Lord, C.F., Gebhardt, M.C., Tomford, W.W., Mankin, H.J., 1988. Infection in bone allografts. Incidence, nature, and treatment. J. Bone Joint Surg. Am. 70, 369–376.

Lyons, F.G., Al-Munajjed, A.A., Kieran, S.M., Toner, M.E., Murphy, C.M., Duffy, G.P., O'Brien, F.J., 2010. The healing of bony defects by cell-free collagen-based scaffolds compared to stem cell-seeded tissue engineered constructs. Biomaterials 31, 9232–9243.

Ma, L., Gao, C., Mao, Z., Shen, J., Hu, X., Han, C., 2003. Thermal dehydration treatment and glutaraldehyde cross-linking to increase the biostability of collagen–chitosan porous scaffolds used as a dermal equivalent. J. Biomater. Sci. Polym. Ed. 861–874.

O'Brien, F.J., Harley, B.A., Yannas, I.V., Gibson, L., 2004. Influence of freezing rate on pore structure in freeze-dried collagen-GAG scaffolds. Biomaterials 25, 1077–1086.

O'Brien, F.J., Harley, B.A., Yannas, I.V., Gibson, L.J., 2005. The effect of pore size on cell adhesion in collagen-GAG scaffolds. Biomaterials 26, 433–441.

Pek, Y.S., Gao, S., Arshad, M.S.M., Leck, K.-J., ying, Y.Y., 2008. Porous collagen-apatite nanocomposite foams as bone regeneration scaffolds. Biomaterials 29, 4300–4305.

Pieper, J.S., Oosterhof, A., Dijkstra, P.J., Veerkamp, J.H., Kuppevelt, V., 1999. Preparation and characterization of porous crosslinked collagenous matrices containing bioavailable chondrotin sulfate. Biomaterials 20, 847–858.

Rho, J.-Y., Kuhn-Spearing, L., Zioupos, P., 1998. Mechanical properties and the hierarchical structure of bone. Med. Eng. Phys. 20, 92–102.

Roeder, R.K., Converse, G.L., Leng, H., Yue, W., 2006. Kinetic effects on hydroxyapatite whiskers synthesized by the chelate decomposition method. J. Am. Ceram. Soc. 89, 2096–2104.

Roeder, R.K., Sproul, M.S., Turner, C.H., 2003. Hydroxyapatite whiskers provide improved mechanical properties in reinforced polymer composites. J. Biomed. Mater. Res. 67A, 801–812.

Schoof, H., Apel, J., Heschel, I., Rau, G., 2001. Control of the structure and size in freeze-dried collagen sponges. J. Biomed. Mater. Res. 58B, 352–357.

Seiler III, J.G., Johnson, J., 2000. Iliac crest autogenous bone grafting: donor site complications. J. South. Orthop. Assoc. 9, 91–97.

Tampieri, A., Celotti, G., Landi, E., Sandri, M., Roveri, N., Falini, G., 2003. Biologically inspired synthesis of bone-like composite: self-assembled collagen fibers/hydroxyapatite nanocrystals. J. Biomed. Mater. Res. 67A, 618–625.

TenHuisen, K.S., Martin, R.I., Klimkiewicz, M., Brown, P.W., 1995. Formation and properties of a synthetic bone composite: hydroxyapatite-collagen. J. Biomed. Mater. Res. 29A, 803–810.

Tierney, C.M., Haugh, M.G., Liedl, J., Mulcahy, F., Hayes, B., O'Brien, F.J., 2009. The effects of collagen concentration and crosslink density on the biological, structural and mechanical properties of collagen-GAG scaffolds for bone tissue engineering. J. Mech. Behav. Biomed. Mater. 2, 202–209.

Trelstad, R.L., 1982. Native Collagen Fractionation. In: Furthmayr, H. (Ed.), Immunochemistry of the Extracellular Matrix. CRC Press, Boca Raton, FL, pp. 31–41.

Wahl, D.A., Sachlos, E., Liu, C., Czernuszka, J.T., 2007. Controlling the processing of collagen-hydroxyapatite scaffolds for bone tissue engineering. J. Mater. Sci. Mater. Med. 18, 201–209.

Wang, R.Z., Cui, F.Z., Lu, H.B., Wen, H.B., Ma, C.L., Li, H.D., 1995. Synthesis of nanophase hydroxyapatite/collagen composite. J. Mater. Sci. Lett. 14, 490–492.

Yunoki, S., Ikoma, T., Tanaka, J., 2010. Development of collagen condensation method to improve mechanical strength of tissue engineering scaffolds. Mater. Char. 61, 907–911.

Yunoki, S., Ikoma, T., Tsuchiya, A., Monkawa, A., Ohta, K., Sotome, S., Shinomiya, K., Tanaka, J., 2007. Fabrication and mechanical and tissue ingrowth properties of unidirectionally porous hydroxyapatite/collagen composite. J. Biomed. Mater. Res. 80B, 166–173.

Zioupos, P., Cook, R.B., Hutchinson, J.R., 2008. Some basic relationships between density values in cancellous and cortical bone. J. Biomech. 41, 1961–1968.